



Institute of Paper Science and Technology

SOUND DISPERSION AND ATTENUATION IN THE THICKNESS DIRECTION OF PAPER MATERIALS

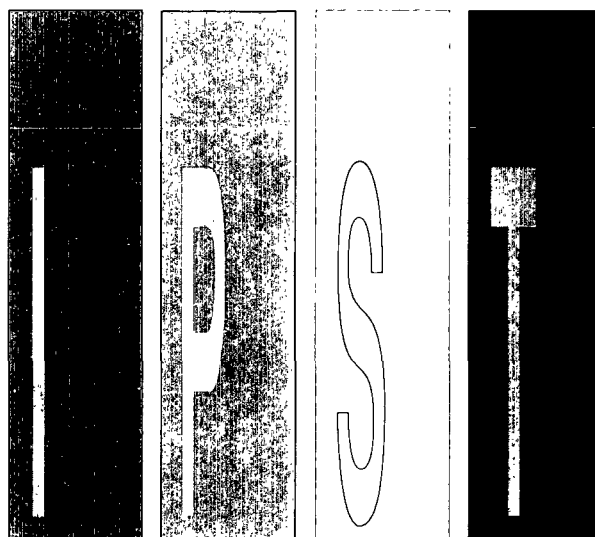
Project 3467

Final Report

to

MEMBER COMPANIES OF THE INSTITUTE OF PAPER SCIENCE AND TECHNOLOGY

June 4, 1992



Atlanta, Georgia

NOTICE & DISCLAIMER

The Institute of Paper Science and Technology (IPST) has provided a high standard of professional service and has put forth its best efforts within the time and funds available for this project. The information and conclusions are advisory and are intended only for internal use by any company who may receive this report. Each company must decide for itself the best approach to solving any problems it may have and how, or whether, this reported information should be considered in its approach.

IPST does not recommend particular products, procedures, materials, or service. These are included only in the interest of completeness within a laboratory context and budgetary constraint. Actual products, procedures, materials, and services used may differ and are peculiar to the operations of each company.

In no event shall IPST or its employees and agents have any obligation or liability for damages including, but not limited to, consequential damages arising out of or in connection with any company's use of or inability to use the reported information. IPST provides no warranty or guaranty of results.

INSTITUTE OF PAPER SCIENCE AND TECHNOLOGY

Atlanta, Georgia

**SOUND DISPERSION AND ATTENUATION IN THE
THICKNESS DIRECTION OF PAPER MATERIALS**

Project 3467

Final Report

A Progress Report

to

MEMBER COMPANIES OF THE INSTITUTE OF PAPER SCIENCE AND TECHNOLOGY

By

Pierre H. Brodeur

June 4, 1992

TABLE OF CONTENTS

LIST OF FIGURES.....	iii
EXECUTIVE SUMMARY.....	iv
INTRODUCTION	1
I. TIME DOMAIN ANALYSIS.....	4
II. FREQUENCY DOMAIN ANALYSIS.....	6
A. Sound Dispersion.....	6
B. Sound Attenuation and Reflection	8
III. EXPERIMENTAL PROCEDURE.....	10
A. Fluid-filled Wheels Setup.....	10
B. Dry Coupling Using Rubber Tires	10
C. Paper Materials.....	12
IV. TIME DOMAIN MEASUREMENTS.....	13
A. Pulse Analysis	13
B. Calibration Procedure	15
C. FFW Paper Thickness	15
D. Thickness Direction Longitudinal Sound Velocity.....	16
V. FREQUENCY DOMAIN MEASUREMENTS.....	18
A. Frequency Analysis	18
B. Phase and Group Velocities	20
C. Elastic Stiffness.....	23
D. Sound Attenuation.....	23
E. Sound Reflection	27
VI. CONCLUSIONS.....	29
ACKNOWLEDGMENTS.....	31
REFERENCES.....	32

LIST OF FIGURES

1. Schematic of the fluid-filled wheels technique (FFW).	4
2. Typical time domain recordings for the reference and specimen directly transmitted pulses #1.	14
3. Recordings of the reference and specimen reflection-delayed pulses #2.	14
4. Fluid-filled wheels thickness as a function of the soft-platen thickness.	16
5. Fluid-filled wheels longitudinal velocity as a function of the soft-platen longitudinal velocity obtained from a reference measurement technique using neoprene-faced PVDF transducers.	17
6. Amplitude spectra for the reference and 69 lb linerboard specimen pulses #1 displayed in Fig. 2.	18
7. Frequency at maximum amplitude versus the fluid-filled wheels thickness.	19
8. Phase spectra for the reference and specimen pulses presented in Fig. 2.	20
9. Phase and group velocities as a function of frequency for the 69 lb linerboard.	22
10. Predicted phase velocity at 1 MHz as a function of the soft-platen velocity.	22
11. Sound attenuation coefficient for the 69 lb linerboard sample as predicted from phase information using the Kramers-Kronig relationship and as directly determined from amplitude measurements when $R_a = 0$ and 0.88.	24
12. Additional examples of sound attenuation coefficient results.	24
13. Graphics depicting the sound attenuation coefficient at 1 MHz as a function of the thickness direction elastic modulus at 1 MHz for linerboards.	26
14. Loss attenuation at 1 MHz as a function of the FFW thickness for medium, linerboard, and heavy board samples.	27
15. Apparent reflection coefficient as a function of the apparent surface roughness.	28

technique. Since the reflection coefficient is obtained under pressure conditions, this quantity might be useful to predict the printing behavior of linerboards and heavier grades. Under reduced pressure conditions, the simultaneous evaluation of the attenuation and reflection coefficients might be used to provide independent measurements of the bulk and surface tissue softnesses, respectively.

INTRODUCTION

Ultrasonic characterization of metals, plastics, and composites is best accomplished by immersion coupling in a water tank or by using a coupling agent such as a viscous fluid or epoxy. For obvious reasons, standard methods of coupling are prohibited for paper materials, and one has to rely on dry coupling. Under this prerequisite, use of contactless methods based on air-coupled transducers or laser-ultrasonics techniques would be the ultimate goal to achieve. However, several difficulties lie ahead in implementing them: rough surfaces, elastic properties sensitive to moisture, and pressure dependent thickness. These techniques have been marginally applied to paper. The remaining alternative is dry-contact coupling which has led to the successful development of NDE ultrasonic techniques especially adapted to paper materials. Techniques are available for in-plane¹ and thickness direction measurements.^{2,3}

Papers are heterogeneous and porous materials made of a complex network of wood fibers. Pore dimensions are strongly related to fiber dimensions (length: 200 to 5000 μm ; diameter 10 to 50 μm). Considering that the paper thickness can be as small as 25 μm , the number of fiber layers can be very small. The fibrous structure of paper indicates that scattering will be the preferential mechanism for sound dispersion and attenuation.

While the primary interest in gathering ultrasonic information from papers concerns the three-dimensional measurement of their elastic stiffness behavior,^{1,2,4-8} a self-contained study of sound dispersion, attenuation, and reflection phenomena is not yet available. Using 2.5 MHz piezoelectric ceramic transducers, neoprene buffers to enhance coupling efficiency, and a 50 kPa loading pressure, dispersion of thickness direction longitudinal waves was studied between 1 and 2 MHz for a limited number of machine-made papers.² It was observed that there is a detectable increase in phase velocity as frequency increases (few percent variation). Neoprene-faced PVDF transducers excited at 1.5 MHz and a loading pressure of 20 kPa were used to evaluate tissue

softness from attenuation measurements.⁹ A pulse-echo method using double-element PVDF transducers was developed to predict sound transmission through paper from reflection measurements at the rubber-paper interface.¹⁰ Because of poor coupling, the measured reflection coefficients were different from those obtained from impedance calculations; for this reason, the technique was not successful.¹¹

On-line through-transmission methods were recently proposed as a mean of evaluating the elastic stiffness properties of a moving paper web in a paper mill.¹² One of these methods, the fluid-filled wheels (FFW) technique, has emerged as a promising candidate for continuous monitoring of thickness direction stiffness properties.¹³ The FFW technique uses stationary piezoelectric ceramic transducers mounted on the axles of fluid-filled rubber wheels in contact with the moving web. With the exception of dry-contact coupling requirements, the FFW transducers' arrangement is similar to the emitter-receiver assembly typically used for immersion testing. In its basic configuration, the FFW technique allows simultaneous determination of paper thickness and traveling time in paper, from which the thickness direction longitudinal sound velocity is evaluated. Since it is relatively straightforward to collect additional information in the frequency domain, the FFW technique can be used to investigate sound dispersion, attenuation, and reflection phenomena. Moreover, it allows the verification of the Kramers-Kronig relationships under dry-contact coupling conditions.

We report in this study the findings of time and frequency domain measurements using a static version of the on-line FFW technique for several machine-made, commercial paper specimens. These papers, which have different mechanical and physical properties, were deliberately chosen to establish some general trends on how sound propagates through the thickness direction of paper. Principles of time domain measurements using the fluid-filled wheels technique are first reviewed. Principles of sound dispersion, attenuation, and reflection measurements in the frequency domain

are introduced. Next, the experimental procedure is described. Measurements are then presented and discussed.

I. TIME DOMAIN ANALYSIS

A schematic of the fluid-filled wheels measurement technique is presented in Fig. 1. Two transducers are mounted on the axles of rubber wheels filled with water. They are stationary and aligned in a transmission mode configuration. The separation distance between them is fixed. Rubber tires are under constant loading pressure to maximize dry-contact coupling efficiency. Thus, the sound path in water is decreased by an amount equivalent to paper thickness when a specimen is inserted in the nip between the wheels. It is assumed that the rubber path length in each wheel does not vary during the insertion process.

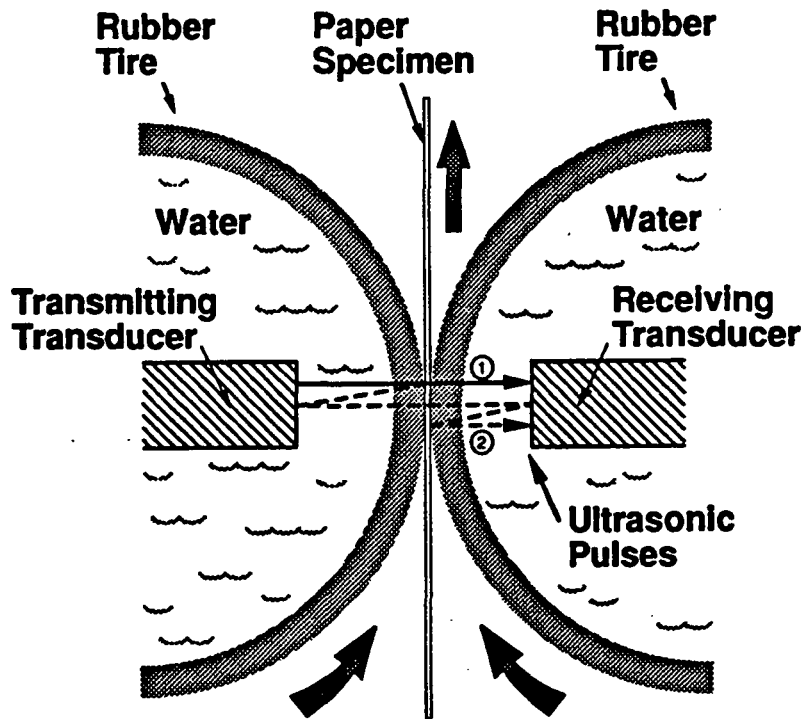


FIG. 1. Schematic of the fluid-filled wheels technique (FFW). The solid and dashed lines correspond to the travel paths for the directly transmitted pulse #1 and reflection-delayed transmitted pulse #2, respectively.

The directly transmitted pulse from the emitter to the receiver is defined as the "reference" pulse #1 when no sample is present in the nip. Otherwise, it is defined as the "specimen" pulse #1 (shown

in Fig. 1). Since the pulse #1 (either reference or specimen) travels through mediums with different impedances, several reflection-delayed pulses are created. Assuming that these pulses do not interfere with each other by an appropriate choice of the tires' rubber thickness and by proper adjustment of the transducers' separation distance and their relative positions with respect to the nip, only a few of them are of practical interest. This is particularly the case for the pulse #2 in Fig. 1. Time delay measurements between pulses #1 and #2 recorded without and with a sample in the nip can be used to determine the sample thickness, h , and the traveling time, t_h , through paper. Mathematical details for the measurement technique are reported elsewhere.¹³ They are summarized here. Providing that the sound velocity in water is given by v_a , it is shown that h is

$$h = v_a [\Delta t_{21} - \Delta t_{2'1'}] / 2 \quad (1)$$

where $\Delta t_{21} = t_2 - t_1$, and $\Delta t_{2'1'} = t_2' - t_1'$ are the time differences between pulses #1 and #2 collected without and with a specimen in the nip, respectively. t_h is described by

$$t_h = \Delta t_{1'1} + h/v_a \quad (2)$$

in which $\Delta t_{1'1} = t_1' - t_1$ is the time difference for the directly transmitted pulse obtained with and without a specimen in the nip. One can note that Eqs. (1) and (2) are independent of the transducers' separation distance and their relative positions with respect to the nip. They are also independent of the traveling time through the rubber tire paths. Because paper thickness is sensitive to the loading pressure in the nip, measurements must be calibrated. This is done by reinterpreting v_a as an apparent sound velocity or, more simply, a calibration factor. In this work, the FFW thickness was calibrated against the so-called soft-platen thickness obtained from a laboratory neoprene platen thickness gauge.¹⁴

From the ratio of Eqs. (1) and (2), the thickness direction (z-axis) longitudinal sound velocity is

$$v_z = h / t_h = 1 / \{ \Delta t_{11} / h + 1/v_a \} \quad (3)$$

v_z is related to the elastic stiffness coefficient, C_{33} , and the sheet apparent density, ρ , such that

$$v_z^2 = C_{33} / \rho \quad (4)$$

II. FREQUENCY DOMAIN ANALYSIS

A. Sound Dispersion

When the velocity of a sound wave propagating through a medium varies as a function of frequency, the medium has dispersive properties. In order to determine the dispersion of a solid specimen, Sachse and Pao¹⁵ proposed a phase measurement technique in which transducers are brought into contact with each other for a reference pulse and then brought into direct contact with the specimen to obtain a specimen transmitted pulse. In the water immersion testing method introduced by Lee et al.,¹⁶ the reference and specimen pulses are obtained without and with the specimen in the water path. This method is an improvement over Sachse's technique which depends on the transducer-sample interface coupling conditions.

Using similarity arguments to Sachse's and Lee's methods, the directly transmitted reference and specimen pulses in the fluid-filled wheels technique can be used to gather dispersion information. Since the impedance of rubber largely exceeds the impedances of air and paper, it is assumed that the coupling conditions at the rubber-air and rubber-paper interfaces are not significantly different. Expressed differently, any phase shift attributed to changing coupling conditions when a specimen is in the nip is small when compared to the specimen phase shift.

Considering that dispersion is negligible in water and rubber at low MHz frequencies, the spectral functions $U_r(\omega)$ and $U_s(\omega)$ for the directly transmitted reference and specimen pulses are respectively¹⁶

$$U_r(\omega) = |U_r(\omega)| \exp[-j\phi_r(\omega)] \quad (5)$$

$$U_s(\omega) = |U_s(\omega)| \exp[-j\phi_s(\omega)] \quad (6)$$

where $|U_r(\omega)|$ and $|U_s(\omega)|$ are the amplitude spectra; $-\phi_r(\omega)$ and $-\phi_s(\omega)$ are the phase spectra; and $\omega = 2\pi f$ is the angular frequency. The net phase produced by the specimen inserted in the nip is

$$\phi(\omega) = -\phi_r(\omega) - [-\phi_s(\omega)] + 2\pi f h / v_a \quad (7)$$

where h is the equivalent paper thickness in the water path. The dispersion relationship described by the propagation constant β is

$$\beta = \phi(\omega) / h = \Delta\phi / h + 2\pi f / v_a \quad (8)$$

in which $\Delta\phi = \phi_s(\omega) - \phi_r(\omega)$ is the phase difference. The phase velocity is given by

$$v_p(f) = \omega / \beta = v_a / [1 + [v_a \Delta\phi / 2\pi f h]] \quad (9)$$

We can also define the group velocity which corresponds to the rate of change of the phase velocity as the incident pulse propagates through the specimen.

$$v_g(f) = d\omega / d\beta = v_a / [1 + [v_a / 2\pi h] [d\Delta\phi / df]] \quad (10)$$

For a nondispersive material, $v_g(f)$ is equal to $v_p(f)$.

B. Sound Attenuation and Reflection

The decrease in amplitude of a sound wave as it propagates through a specimen is described as sound attenuation. This phenomenon is usually attributed to absorption, which relates to the material structure, and/or to scattering, which relates to the material component dimensions with respect to the ultrasonic wavelength. In a typical transmission arrangement involving immersion coupling, the amplitude of the transmitted pulse through a specimen is a function of sound attenuation and reflectivity at the water-specimen boundary. For the fluid-filled wheels technique, a complication arises from the dry-contact coupling conditions. This difficulty can be alleviated by defining an apparent reflection coefficient, R_a . This coefficient is a priori unknown. Neglecting sound attenuation in water and rubber, it can be shown that¹⁶

$$\alpha(f) = -\ln \left[\frac{U_s(f) / U_r(f)}{[1 - R_a^2]} \right] / h \quad (11)$$

in which $U_s(f) / U_r(f)$ is the amplitude ratio of the specimen and reference pulses. The loss attenuation is given as the product of $\alpha(f)$ by the thickness h .

Since an acoustic medium is a causal system, the attenuation coefficient is related to the phase velocity by the Kramers-Kronig relationships. In other words, sound attenuation as a function of frequency can be predicted from dispersion and vice versa. Assuming that the phase velocity does not vary rapidly with frequency (absence of sharp resonance), the nonlocal Kramers-Kronig relationships can be approximated by nearly local relations.¹⁷ In that particular situation, a simple expression for the attenuation coefficient is obtained:

$$\alpha(\omega) = [\pi\omega^2 / 2v_p^2(\omega)] dv_p(\omega) / d\omega \quad (12)$$

III. EXPERIMENTAL PROCEDURE

A. Fluid-filled Wheels Setup

Referring to Fig. 1, two identical, unfocused, immersion-type, broadband piezoelectric ceramic transducers from Panametrics were used to launch and receive ultrasonic pulses. They were mounted on the axles of identical fluid-filled wheels obtained from Dapco Industries. $\lambda/20$ faceplates were specified to reduce pulse #2 distortion; this was caused by interfering reflections at the ceramic-faceplate interfaces. The transducers' nominal resonant frequency and active area diameter were 1 MHz and 19 mm, respectively. Their separation distance and the ratio of their relative positions with respect to the nip were set to approximately 9.5 cm and 0.67, respectively. Although asymmetric, the FFW transmitter-receiver configuration was shown to be reciprocal.

A 1 MHz, one-cycle sine wave was used to excite the transmitter. The pulse amplitude was varied from 10 V_{RMS} for reference measurements to 200 V_{RMS} for thick specimen measurements in order to improve the signal-to-noise ratio. Incident and transmitted amplitudes were linearly related for all tested specimens. Received pulses were detected with a 34 dB preamplifier and captured on a one-to-one basis with a GPIB-controlled 2432 Tektronix scope. Signal averaging (32 successive acquisitions) was used to further improve the S/N ratio. Collected pulses were transferred to a 386 computer for later analysis. A cross-correlation procedure was used in combination with a second-order interpolation routine to achieve a time resolution better than 5 ns. All measurements were performed at 50% relative humidity and 23 °C in a controlled environment.

B. Dry Coupling Using Rubber Tires

As paper materials have rough surfaces, dry-contact coupling efficiency can be optimized by using conformable rubber layers between ultrasonic probes and paper.³ In this work, molded urethane (hard rubber) and natural rubber (soft rubber) tires having an outer diameter of 16.5 cm and a

width of 6 cm were tested on a comparative basis to determine the best coupling conditions. A 7.9 mm tire thickness was chosen to avoid interference from unwanted reflections at rubber-water boundaries inside the wheels. Water pressure was set to 50 kPa.

Preliminary observations with molded urethane tires indicated that the directly transmitted reference pulse amplitude was increased when the loading pressure at the nip interface was increased. This was achieved by decreasing the separation distance between the wheels' axles (few millimeters range). Below a critical distance, the pulse amplitude was observed to remain constant. This was attributed to the contact area exceeding the ultrasonic beam cross section. As a compromise to avoid excessive pressure, the separation distance was set to be slightly lower than the critical distance. It was not modified when soft tires were used. Using an ultrasuper low pressure measurement film composed of a layer of microcapsulated color-forming material (Fuji film), it was verified that the contact area between the hard tires was increased when the sample thickness was increased. This led to the assumption that the nip interface pressure did not significantly vary as a function of sample thickness for these tires. It was estimated to be less than 200 kPa, i.e., the lowest measurable pressure with pressure films. This is four times higher than the 50 kPa loading pressure used to determine the soft-platen thickness.¹⁴ The nip interface pressure could not be determined for soft tires.

Under wet coupling conditions with a thin film of water in the nip, no significant difference in the reference pulse amplitude was observed for hard and soft tires. Under dry coupling conditions, the pulse amplitude was nearly twice as large for soft tires. Using a pulse-echo technique, reflected pulses at the incident rubber-paper interface were sensitive to the presence of paper specimens with soft tires only. While these facts supported a better coupling efficiency for soft tires (better conformability), transmission measurements with increasingly thicker paper samples showed that the specimen pulse amplitude deteriorated less rapidly with hard tires. This unexpected contradiction was attributed either to enhanced coupling efficiency or to decreased

attenuation in the specimens due to consistently higher loading pressure with hard tires. Because of the better sound transmission through thick papers, it was decided to use molded urethane tires for most of the experimental work. This choice was further supported by the general observation of interference-free amplitude spectra for specimens evaluated with hard tires; this was not the case when soft tires were used. At maximum available input power, transmitted pulses were detected through specimens as thick as 1.75 mm. In order to maintain as constant as possible coupling conditions, specimens were inserted in the nip by rotating the tires to a specific angular position instead of opening the gap between the wheels. Unless otherwise specified, only those measurements obtained with hard tires are reported.

C. Paper Materials

A total of 29 machine-made, commercial paper specimens ranging from 40 to 1750 μm were tested. They were divided into four distinct categories: "Fine Papers" which represent specimens under 100 μm , i.e., copier, writing, and draft papers, and newsprints; "Corrugating Mediums" which are lightweight paperboards used for the fluted inner plies of corrugated boxboards (175 to 325 μm); "Linerboards" which are paperboards used as facings of corrugated boxboards (250 to 875 μm); "Heavy Boards" referring to thick paperboards and cardboards (500 to 1750 μm). These papers have diversified mechanical and physical properties due to different formation parameters, different furnishes, and different fiber dimension distributions. Of the four categories, linerboards provided the most homogeneous subset. Specimens were tested in a random order.

IV. TIME DOMAIN MEASUREMENTS

A. Pulse Analysis

Typical pulses collected without and with a specimen in the nip are displayed in Fig. 2 (reference and specimen pulses #1) and Fig. 3 (reference and specimen pulses #2). All amplitudes are relative to the reference pulse #1 amplitude in Fig. 2. The paper sample selected for the purpose of illustrating measurements is a nominal 69 lb linerboard (69 lb corresponds to a basis weight of 69 lb/1000ft² or 337 g/m²). Several observations can be denoted. The time delay between pulses #1 or #2 (either reference or specimen) is approximately 128 μ s; this is about twice the traveling time between the transducers. Specimen pulses are delayed with respect to reference pulses. This is a consequence of the smaller sound velocity in paper (typically from 150 to 500 m/s) when compared to the sound velocity in water. Amplitudes for pulses #2 are eight times less than amplitudes for pulses #1. Considering that the former pulses are subjected to four successive reflections, the eightfold decrease is relatively small.

Pulses crossing specimens more than one time were not observed. Without ruling out the possibility of sound reverberation in some of the specimens (especially if the thickness is less than the acoustic wavelength), pulse distortion due to multiple internal reflections was not detected. In order to evaluate the possible effects of internal reflections on the thickness and traveling time measurements (Eqs. 1 and 2), preliminary measurements were carried out with aluminum shims under dry coupling conditions. Although pulse distortion was unavoidable for aluminum at less than 1 MHz, results demonstrated that thickness measurements for shims ranging from 80 μ m to 750 μ m were not affected by internal reflections that could not be discriminated. This pointed to similar reverberation-related dispersion for specimen pulses #1 and #2. Traveling time measurements were not as successful because "distorted" specimen pulses #1 could not be properly correlated to a "nondistorted" reference pulse #1. From these observations, it was

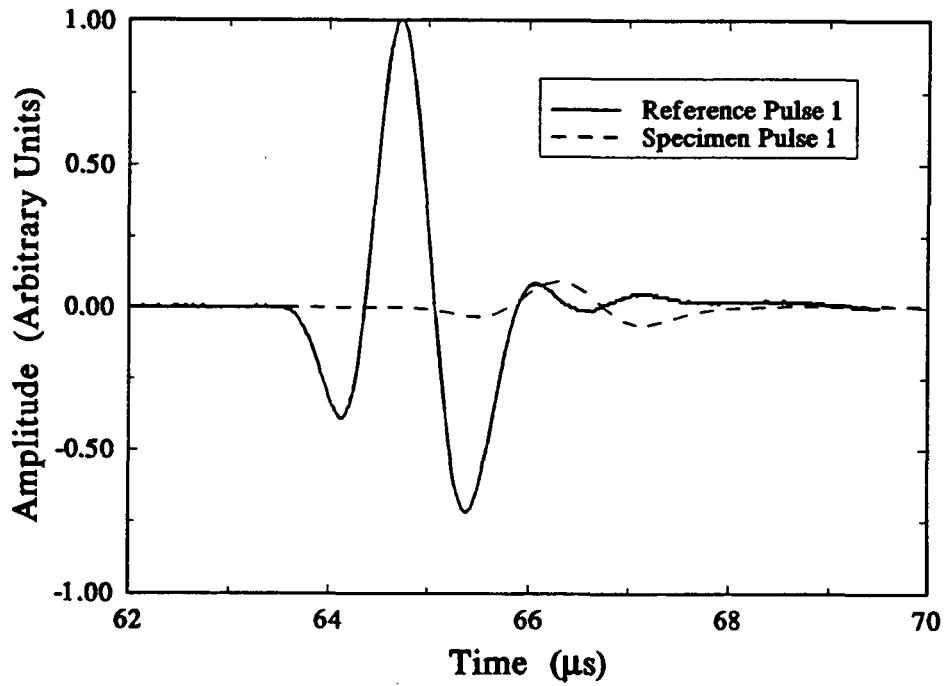


FIG. 2. Typical time domain recordings for the reference and specimen directly transmitted pulses #1. The specimen pulse was recorded for a 461 μm thick 69 lb linerboard.

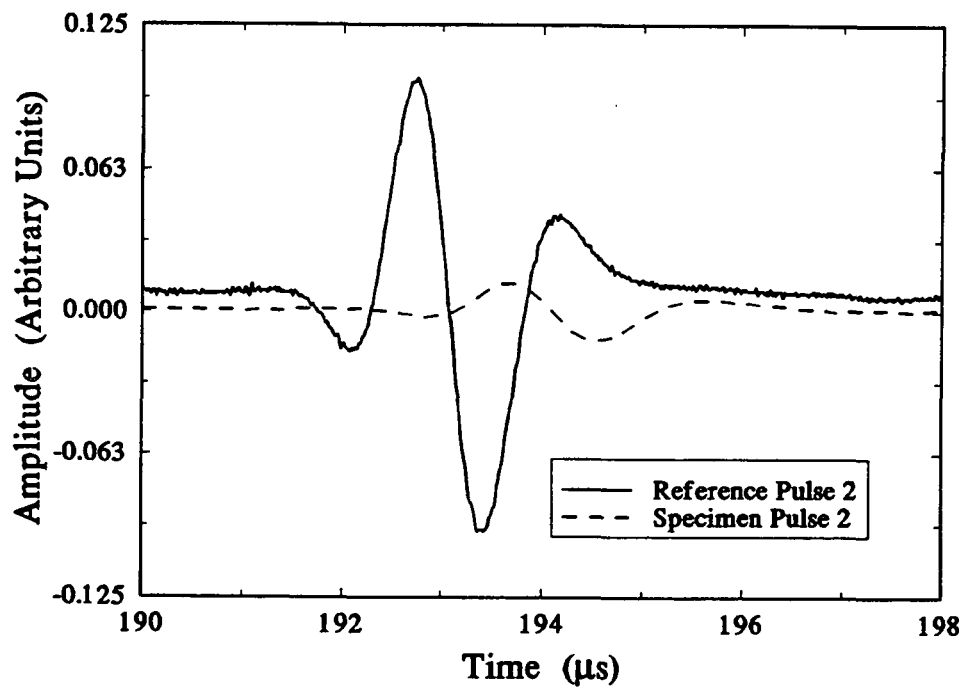


FIG. 3. Recordings of the reference and specimen reflection-delayed pulses #2.

concluded that the presence of internal reflections (if any) was an unlikely factor to affect paper thickness evaluation. However, traveling time measurements may be affected.

B. Calibration Procedure

As previously mentioned, the FFW thickness was calibrated against the soft-platen (SP) thickness.¹⁴ All 29 paper specimens were used for that purpose. As a first step, the apparent velocity v_a was determined for each specimen, assuming a known SP thickness h in Eq. (1). Then, the mean apparent velocity was computed; it was defined as the calibration factor. This procedure was repeated for three independent sets of data. In this manner, v_a was found to be 1523 ± 51 m/s.

C. FFW Paper Thickness

In conjunction with cross-correlation calculations involving full-length pulses, Eq. 1 was used to evaluate the FFW thickness for three sets of measurements. Results are presented in Fig. 4 as a function of the SP thickness. The accuracy is 9% when all specimens are considered; it is 7.4% when fine papers are excluded. A close look at the data shows that some of the sample thicknesses are more pressure sensitive than others, thus affecting accuracy. Nevertheless, the relationship is linear. Contrary to expectations, the accuracy was also affected by pulse #2 distortion which could not be sufficiently eliminated (see Sect. III A). This was demonstrated by repeating cross-correlation calculations with truncated pulses (first-half cycle). In doing so, the accuracy was particularly improved for fine papers, leading to an overall accuracy of 4.7%. Thus, best thickness measurements using the FFW technique were obtained when pulses were truncated. Accuracy could further be enhanced by determining a calibration factor for each category of papers and by increasing the number of measurements per specimen.

Within experimental errors, there is a good correlation between FFW and SP velocities for linerboards and heavy boards. Medium velocities do not correlate so well, and poor agreement is denoted for four of the six fine paper velocities. Thickness inaccuracies seen in Fig. 4 for some of the fine papers do not support large velocity discrepancies for these specimens. Two explanations are proposed: velocity measurements are dispersion sensitive, and a slight difference in the frequency content of the reference pulse in both methods of measurements will primarily affect fine paper measurements; coupling differences in the FFW setup when a sample is or is not present in the nip are such that the frequency content of the fine paper pulses is generally higher than its counterpart for the reference pulse, thus leading to potentially erroneous calculations. This second explanation is further discussed in the next section.

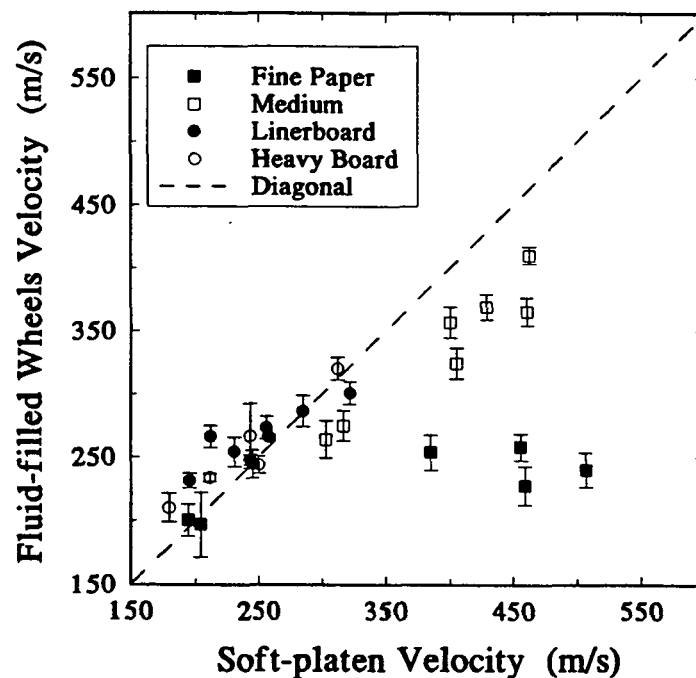


FIG. 5. Fluid-filled wheels longitudinal velocity as a function of the soft-platen longitudinal velocity obtained from a reference measurement technique using neoprene-faced PVDF transducers. The first-order curve fitting excludes fine paper data points.

V. FREQUENCY DOMAIN MEASUREMENTS

A. Frequency Analysis

A fast Fourier transform procedure was used to evaluate the frequency content of the directly transmitted reference and specimen pulses (Fig. 2). Amplitude spectra U_r and U_s are depicted in Fig. 6. The frequency at maximum amplitude for the reference pulse is 0.70 MHz. This is less than the 0.74 MHz frequency obtained under wet coupling conditions. For comparison, results gathered with soft rubber tires show that the frequency for dry and wet coupling is 0.74 and 0.78 MHz, respectively. Also, the measured resonant frequency for the 1 MHz transducers is 0.87 MHz. Because the 0.04 MHz frequency difference between wet and dry coupling does not vary for different rubber materials, it is postulated that the use of rubber tires in the FFW setup is a determinant factor in the transducers' bandwidth downshift. This has serious consequences because it is of no avail to use higher frequency transducers (e.g., 2.25 MHz) to improve time resolution or to study dispersion and attenuation. The shift toward a lower frequency (0.46 MHz)

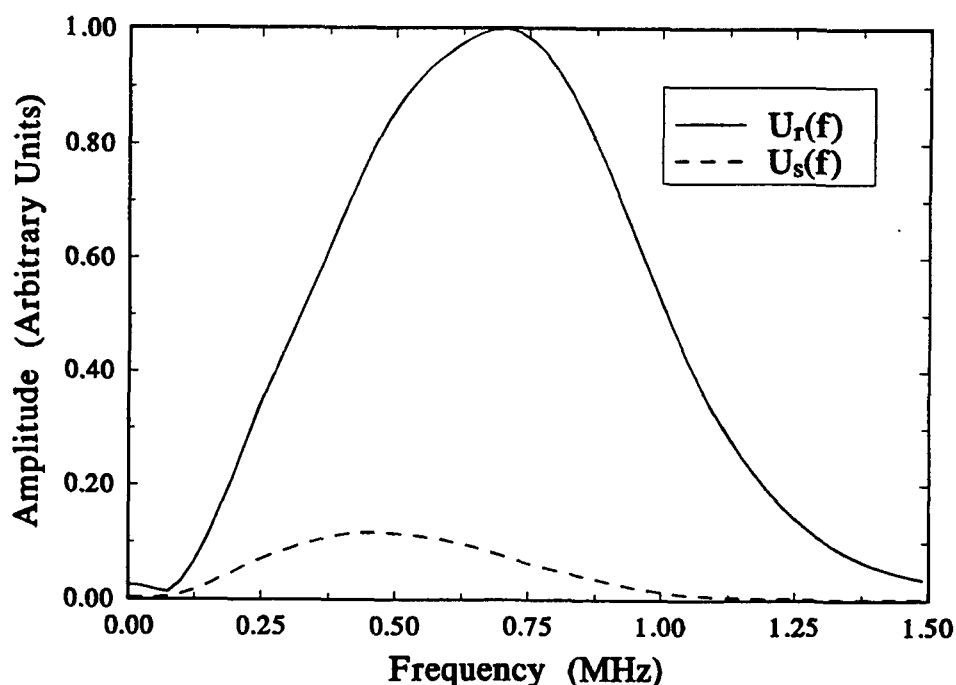


FIG. 6. Amplitude spectra for the reference and 69 lb linerboard specimen pulses #1 displayed in Fig. 2.

for the 69 lb linerboard specimen frequency is a manifestation of dispersion in paper.

The frequency at maximum amplitude was determined for all specimens. This is shown in Fig. 7 as a function of the FFW thickness. The reference frequency (0.70 MHz) is marked by the arrow. In general, it is observed that the frequency is inversely related to the thickness. Moreover, distinct relationships can be established for each paper category, supporting substantially different formation processes and fibrous structures. Qualitative curve fitting extrapolations for medium, linerboard, and heavy board specimens predict a zero thickness frequency higher than the reference frequency and closer to the frequency obtained under wet coupling conditions (0.74 MHz). Since the fine paper frequencies are generally higher than the reference frequency, it is hypothesized that acoustic coupling is somehow improved by inserting paper in the nip even though there are two

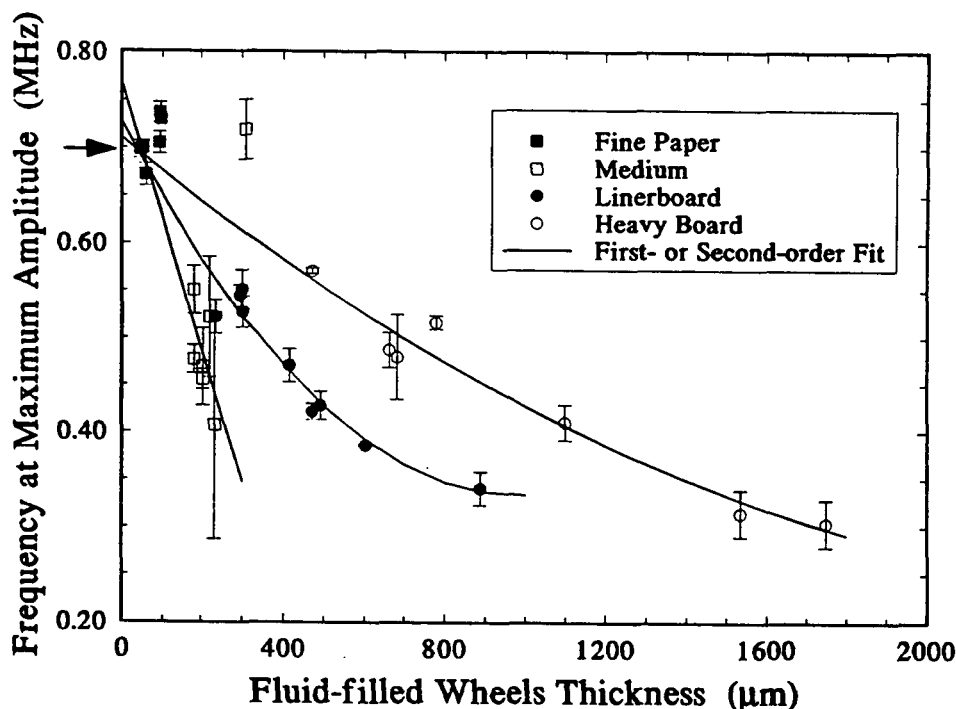


FIG. 7. Frequency at maximum amplitude versus the fluid-filled wheels thickness. The arrow indicates the frequency at maximum amplitude for the reference pulse. The abnormally high frequency associated with one of the medium samples was erroneously computed due to an unexplained large interfering component in the amplitude spectrum for this sample; it was not included in the first-order curve fitting for mediums.

rubber-paper interfaces instead of one rubber-rubber interface. The lower than expected reference frequency was defined as the "reference frequency anomaly." This anomaly impairs the observation of internal reflections. The idea of substituting the "dry" reference pulse by a "wet" reference pulse was investigated, but abandoned due to dramatically different coupling conditions.

B. Phase and Group Velocities

Phase spectra for pulses shown in Fig. 2 are presented in Fig. 8. The larger negative slope for the specimen phase (ϕ_s) is in agreement with a longer traveling time in paper. The relative linearity of the specimen phase with respect to the reference phase (ϕ_r) sustains a weak dispersion in the test-case specimen. In order to compute the phase and group velocities (Eqs. 9 and 10) from the phase difference $\Delta\phi$, a second-order polynomial curve fitting procedure was applied to $\Delta\phi$ (same procedure for all samples).¹⁶ Only data points within an adjustable frequency window were used in the calculations to avoid complications from poor signal-to-noise ratio below 0.25 MHz and

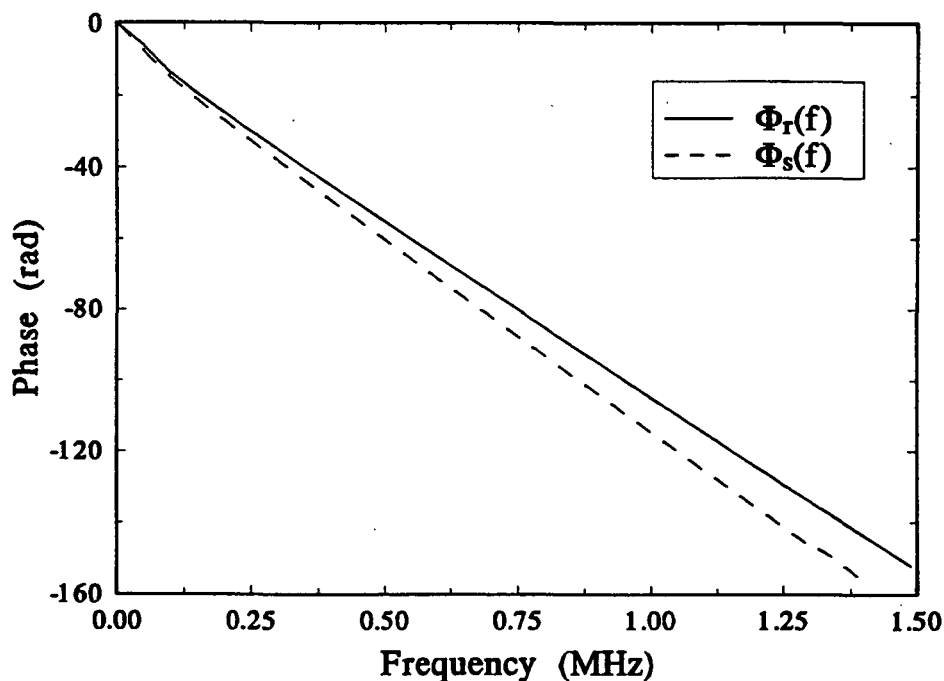


FIG. 8. Phase spectra for the reference and specimen pulses presented in Fig. 2.

above an upper frequency limit which was set to 1.25 MHz for the 69 lb linerboard. From physical considerations, the phase difference intercept was reset to zero.

The phase and group velocities for the 69 lb linerboard are presented in Fig. 9. The phase velocity increases approximately linearly by 7% from 0.25 to 1.25 MHz, confirming a weak dispersion in this frequency range. For comparison, the time domain longitudinal velocity is included in the graph. It is shown to agree within experimental error. Dispersion is evident from the discrepancy between the phase and group velocities.

The phase velocity spectrum was determined for all samples. Figure 10 depicts the phase velocity at 1 MHz as a function of the time domain FFW velocity for mediums, linerboards, and heavy boards. Calculations for fine papers could not be handled properly due to the reference frequency anomaly. Dispersion did not exceed 10% from 0.25 to 1.25 MHz, and no relationship between dispersion and thickness was noted. This is in agreement with previous findings by Habeger and Wink.² A comparative analysis of Figs. 5 and 10 shows that the time domain and phase velocities for linerboard and heavy boards are in good agreement; this is not the case for mediums.

Without considering sound reverberation, the reference frequency anomaly does not permit the evaluation of reliable phase velocities for specimens thinner than approximately 200 μm . This limit is based on experimental observation. The extent of the unreliability is hard to appraise. Even though time domain FFW velocities can be determined below 200 μm , they do not correlate with time domain SP velocities. Since calibrated velocities are as yet unavailable for papers, SP velocities cannot be verified as well. Consequently, the validity of thickness direction longitudinal velocity measurements for thin papers remains an open question. The difficulty could be resolved by testing specimens of various thicknesses but of uniform thickness direction properties. However, the formation of handmade papers having a thickness independent density profile is a very demanding task because paper formation is generally thickness sensitive.

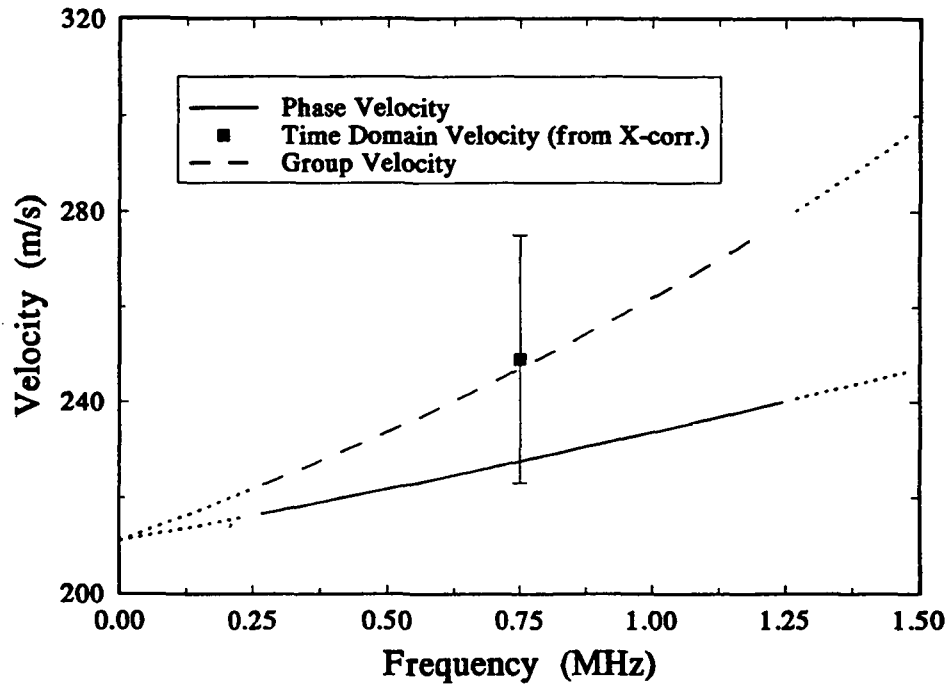


FIG. 9. Phase and group velocities as a function of frequency for the 69 lb linerboard. The time domain longitudinal velocity is shown for comparison.

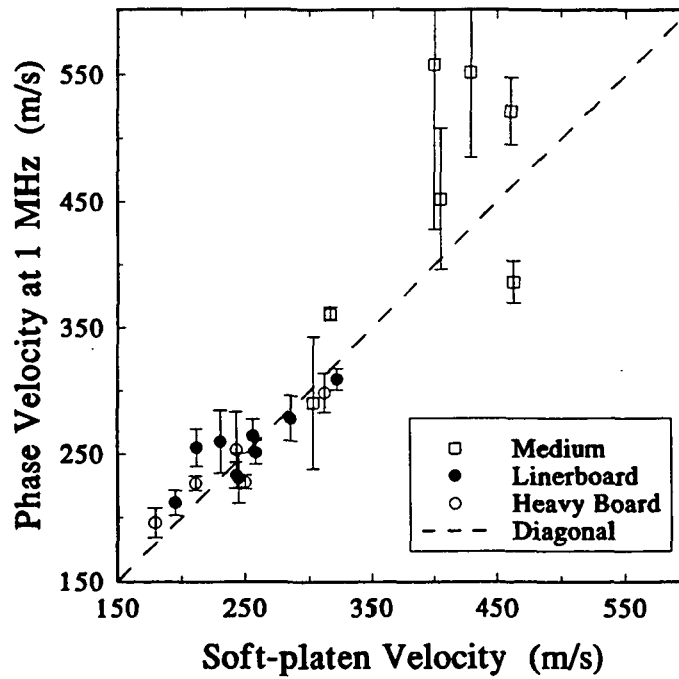


FIG. 10. Predicted phase velocity at 1 MHz as a function of the soft-platen velocity. Results are presented for mediums, linerboards, and heavy boards only.

C. Elastic Stiffness

By replacing v_z with $v_p(f)$ in Eq. (4), the elastic stiffness can be evaluated as a function of frequency. Assuming an apparent sheet density of 712 kg/m^3 , the predicted elastic stiffness C_{33} at very low frequencies (e.g., 1 Hz range) for the 69 lb linerboard sample is approximately 32 MPa. In order to examine this prediction, thickness direction tensile strength measurements were performed. The tensile strength was obtained from samples clamped with double-sided tape (the alternative use of epoxy clamping is unsatisfactory because specimen properties can be altered). An average tensile strength of 290 kPa was measured, i.e., approximately two orders of magnitude less than C_{33} . The most likely reason for this discrepancy is that paper is a viscoelastic material, and as such, relaxation effects at 1 Hz and 1 MHz are completely different. In other words, extrapolation to low frequencies for measurements captured in the 1 MHz range is meaningless. This argument is in agreement with previous, but unrelated, in-plane studies showing that the elastic moduli measured sonically are significantly higher than the load-elongation moduli.^{6,18} When formation processes such as wet pressing, wet straining, and drying restraints are varied for particular handmade and machine-made papers, C_{33} and the tensile strength are known to correlate.⁸ This relationship was not verified for different papers in this study.

D. Sound Attenuation

Using the Kramers-Kronig relationship (Eq. 12) and the phase information, the phase-predicted attenuation coefficient as a function of frequency was computed for the 69 lb linerboard. This is indicated by the solid line in Fig. 11. Results are in decibel per micrometer. Equation 11 and the amplitude spectra shown in Fig. 6 were also used to evaluate the amplitude-determined attenuation coefficient. The long-dashed and short-dashed lines in Fig. 11 represent this coefficient when R_a is set to zero and 0.88, respectively. R_a was taken as the average apparent reflection coefficient within the 0.25 to 1.25 MHz frequency window, on the experimental basis that it was frequency

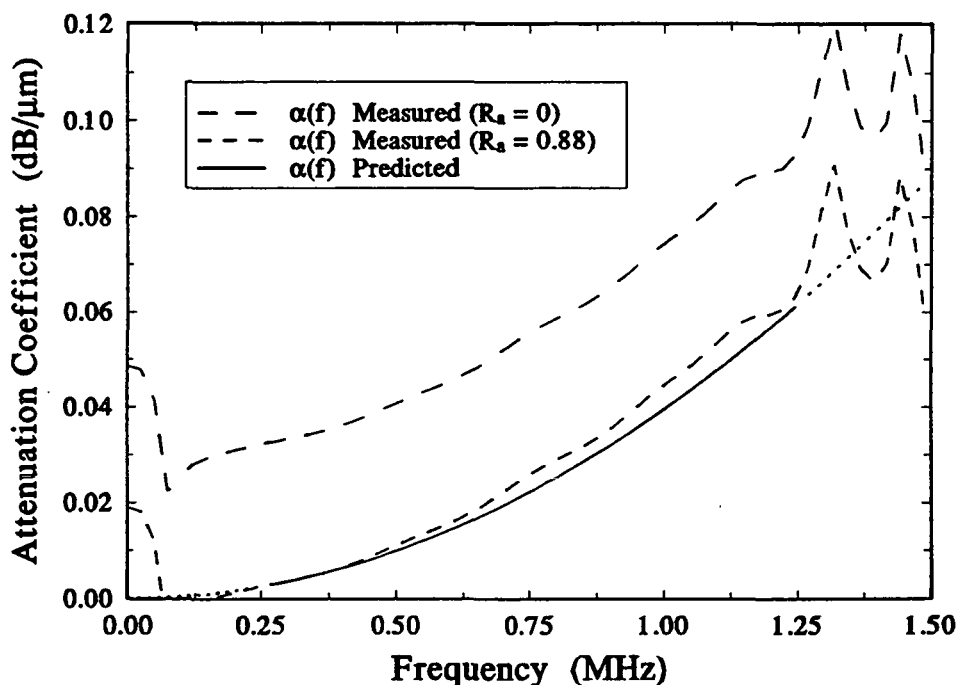


FIG. 11. Sound attenuation coefficient for the 69 lb linerboard sample as predicted from phase information using the Kramers-Kronig relationship and as directly determined from amplitude measurements when $R_a = 0$ and 0.88.

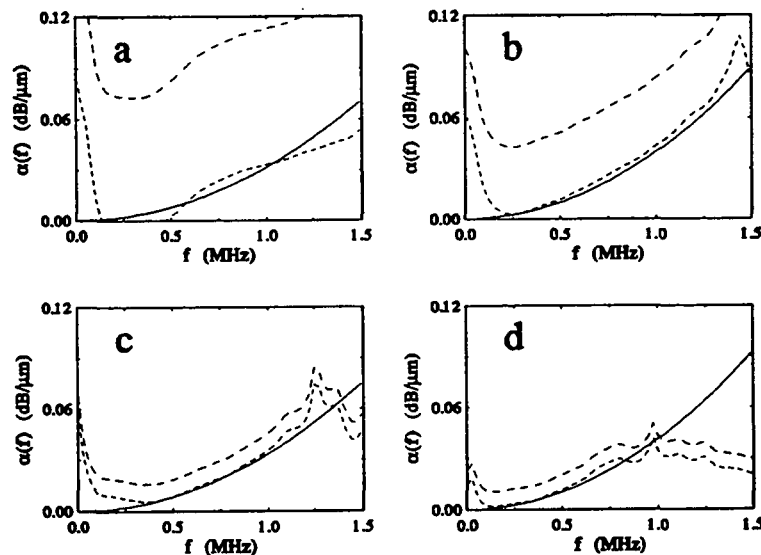


FIG. 12. Additional examples of sound attenuation coefficient results: a) 26# medium (185 μm); b) 42# linerboard (267 μm); c) Tablet board (696 μm); d) Thick solid board (1553 μm).

independent. Equation 14 was used to calculate R_a as a function of frequency. Since the correlation is good between the amplitude- and phase-determined attenuation coefficients, extrapolation to higher frequencies is possible. However, frequency bandwidth limitations in the FFW setup did not allow verification of the predicted attenuation coefficient above 1.5 MHz. The apparent reflection coefficient is high, in agreement with prevailing dry coupling conditions.

The amplitude- and phase-determined attenuation coefficients versus the frequency were obtained for all medium, linerboard, and heavy board specimens. Some examples are illustrated in Fig. 12. Poor correlation for the medium sample (a) is attributed to the reference frequency anomaly. Effects from this anomaly are less and less pronounced as the thickness is increased (especially above 200 μm). Approximate sound transmission cut-off frequencies for the tablet board (c) and thick solid board (d) are 1.2 and 0.8 MHz, respectively. Corresponding acoustic wavelengths for these specimens are 232 and 348 μm . Relationships to the average fiber dimensions were not analyzed. Attenuation results shown in Figs. 11 and 12 confirm that a second-order curve fitting procedure for $\Delta\phi$ is adequate in the sound attenuation prediction scheme using Kramers-Kronig relationships.

Additional insight about the behavior of sound attenuation in paper was obtained by investigating relationships between the phase-predicted attenuation coefficient at 1 MHz, thickness direction elastic modulus at 1 MHz, apparent density, and air permeability. For linerboard specimens, it was found that the attenuation coefficient was inversely related to the elastic modulus (Fig. 13). This relation is consistent with more uniform (homogeneous) mechanical and physical properties for this category of papers. Without assessing a general trend, this seems to demonstrate that the stiffer a paper, the weaker the sound attenuation. Since a stiffer paper is probably less porous, this supports the hypothesis that scattering is the preferential mechanism for sound attenuation in paper. The attenuation coefficient versus the elastic modulus at constant frequency is interesting because it

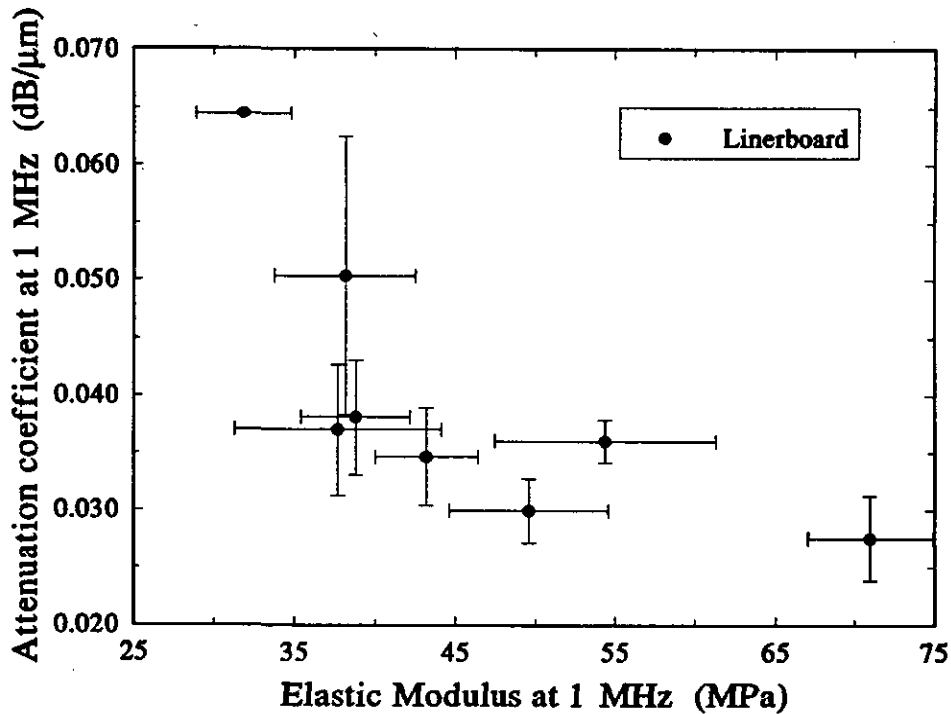


FIG. 13. Graphics depicting the sound attenuation coefficient at 1 MHz as a function of the thickness direction elastic modulus at 1 MHz for linerboards.

implies that mechanical properties may also be inferred from sound attenuation measurements for a particular paper subjected to variable formation conditions.

No correlation was observed between the attenuation coefficient and the apparent sheet density for different papers. A similar conclusion was reached with air permeability as determined using the Bendtsen air permeability technique. Air permeability is a property which is obtained by measuring the rate of flow of air into the fiber network; it is sensitive to coating materials and fillers (if any). It is different from porosity which relates to the ability of fluids (e.g., mercury) to pass into the fiber network. Porosity measurements were not performed.

While the sound attenuation coefficient could not be easily correlated to some of the physical properties of paper, a linear relationship between the loss attenuation (at 1 MHz) and the FFW thickness was found (Fig. 14). Since, the number of fiber layers generally increases as a function of thickness, it is an important contributing factor to sound attenuation. It further supports the sound scattering hypothesis. The loss attenuation is approximately 35 dB for a 1 mm thick paper at 1MHz.

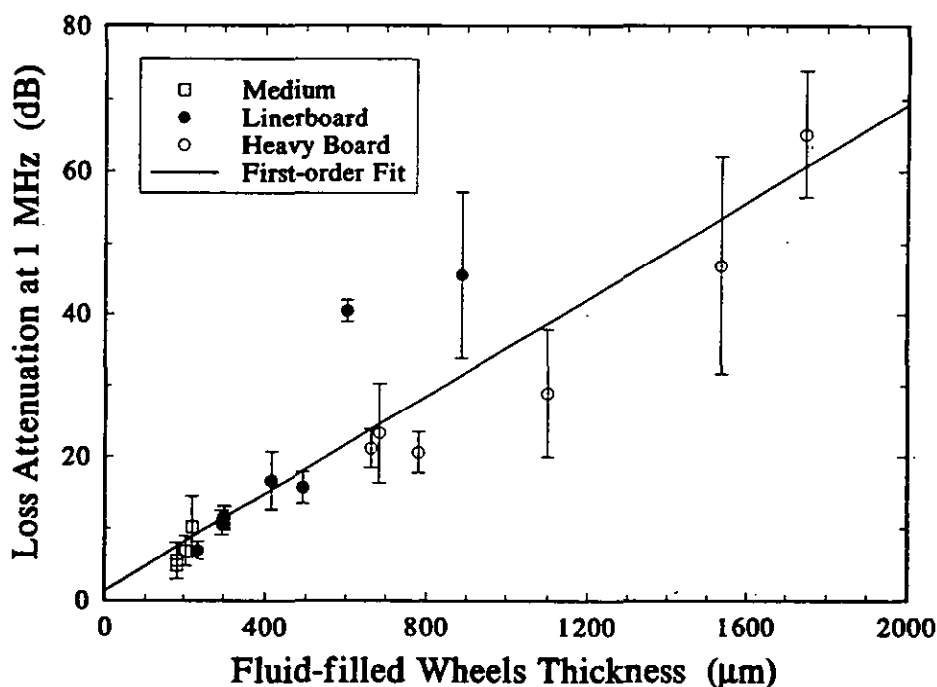


FIG. 14. Loss attenuation at 1 MHz as a function of the FFW thickness for medium, linerboard, and heavy board samples. The dashed line is a first-order curve fitting ($R^2 = 0.84$).

E. Sound Reflection

As a final investigation, the relationship between the apparent reflection coefficient and the apparent surface roughness was examined. The latter quantity is defined in this study by the average of the wire and felt side surface roughnesses, as independently obtained using the Bendtsen roughness method. This method relates surface roughness to the rate of escape of air from under the narrow rim of a bell-shaped head resting on a specimen. As presented in Fig. 15, it appears that the

rougher (or less smooth) the apparent surface, the larger R_a . Wire and felt side roughnesses were generally similar for the specimens investigated in this work. Since the reflection coefficient could not be obtained from pulse-echo analysis for hard rubber tires, the above results are particularly informative.

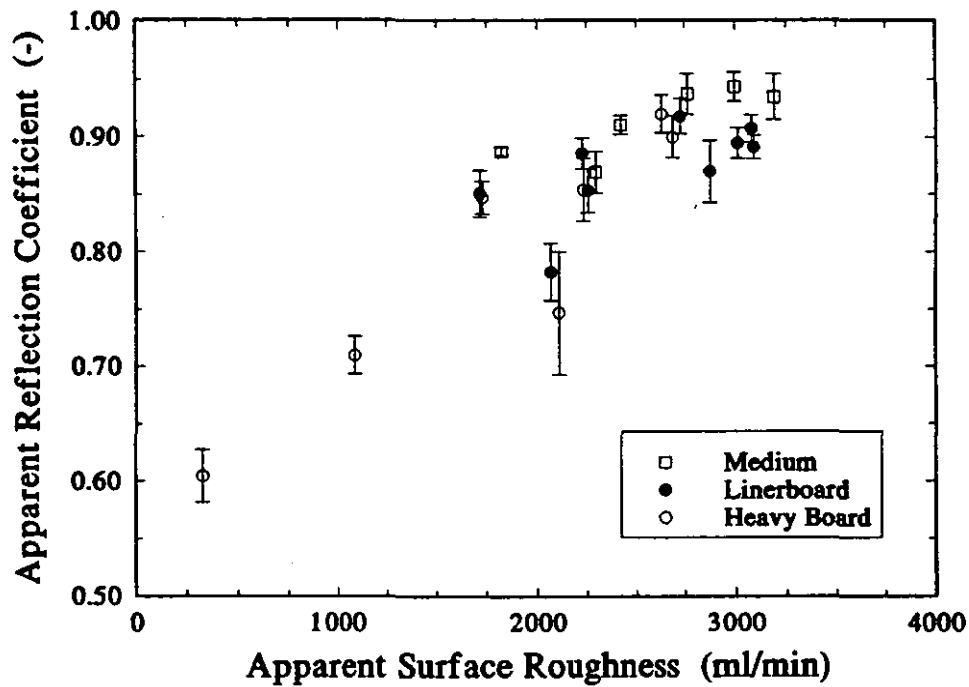


FIG. 15. Apparent reflection coefficient as a function of the apparent surface roughness.

VI. CONCLUSIONS

A through-transmission, dry-contact ultrasonic technique using fluid-filled molded urethane wheels was used to investigate sound propagation in the thickness direction of paper. Several machine-made paper specimens classified into four distinct categories were tested. The paper thickness was determined over a large thickness range. Meaningful longitudinal velocity measurements were obtained for specimens thicker than 200 μm (especially, linerboards and heavy boards). Below this limit, results were sensitive to the reference frequency anomaly. This anomaly was due to the dry-contact coupling conditions which are different when a sample is or is not present in the nip between the wheels. Since the dispersion was generally weak between 0.25 and 1.25 MHz for different papers (less than 10%), measurement of the time domain velocity is a satisfactory approximation to the phase velocity.

The sound attenuation coefficients, as determined directly using amplitude information and indirectly using Kramers-Kronig relationships, were generally in good agreement for specimens thicker than 200 μm . Thus, Kramers-Kronig relationships were verified under dry-contact coupling conditions for paper materials thicker than 200 μm . Due to the FFW frequency bandwidth limitation, measurements could not be gathered above 1.5 MHz. For homogeneous papers, the attenuation coefficient was found to be inversely related to the elastic stiffness at constant frequency. No correlation was established among the sound attenuation coefficient, apparent sheet density, and air permeability for different papers. The loss attenuation was linearly related to the sample thickness, meaning that the number of fiber layers plays a significant role in sound attenuation through paper. The apparent reflection coefficient obtained by comparing the amplitude- and phase-determined sound attenuation coefficients appeared to be inversely related to the apparent surface roughness of paper.

The FFW technique has been proposed to investigate the thickness direction elastic stiffness properties of a moving paper web. The present study shows that it can be used for a wide range of paper materials. Improvement of coupling conditions could further extend its range of applicability to paper thinner than 200 μm and to frequencies higher than 1.5 MHz. Experiments with known furnishes, fiber dimensions, and formation parameters are necessary to fully appreciate the sound dispersion and attenuation phenomena and to provide a better understanding of the structure of paper.

The FFW setup can be modified to sustain high temperature and relative humidity and thus study thickness direction stiffness properties (including thickness) as a function of temperature and relative humidity. Continuous sensing of mechanical properties such as internal bond strength and compressibility and defects such as sheet delamination might be achieved by investigating sound attenuation rather than elastic stiffness. Sound attenuation might also be sensitive to the filler content of paper. While the apparent reflection coefficient could be used to monitor surface roughness under mechanical pressure conditions, a better approach to single-sided surface roughness monitoring would be to evaluate the reflection coefficient using a pulse-echo technique and soft-rubber, conformable tires. Since the reflection coefficient is obtained under mechanical pressure conditions, it might be useful to predict the printing behavior of linerboards and heavier grades. Under reduced pressure conditions, the simultaneous determination of the attenuation and reflection coefficients might be used to provide independent measurements of the bulk and surface tissue softnesses, respectively.

ACKNOWLEDGMENTS

It is a pleasure to thank Dr. Charles C. Habeger from James River Corporation and Prof. Maclin S. Hall for useful discussions. The technical assistance of T.G. Jackson and C. Esworthy is appreciated. This research was supported by the member companies of the Institute of Paper Science and Technology and by the U.S. Department of Energy under contract No. DE-AC05-86CE40777.



Pierre H. Brodeur
Assistant Professor of Physics
Institute of Paper Science and Technology

REFERENCES

- 1 M. Van Zummeren, D. Young, C. Habeger, G. Baum, and R. Trevelen, *Ultrasonics* **25**, 288-294 (1987).
- 2 C.C. Habeger and W.A. Wink, *J. Appl. Pol. Sc.* **32**, 4503-4540 (1986).
- 3 C.C. Habeger, W.A. Wink, and M.L. Van Zummeren, *J. Acoust. Soc. Am.* **84**(4), 1388-1396 (1988).
- 4 G.A. Baum and L.R. Bornhoeft, *Tappi J.* **62**(5), 87-90 (1979).
- 5 R.W. Mann, G.A. Baum, and C.C. Habeger, *Tappi J.* **62**(8), 115-118 (1979).
- 6 R.W. Mann, G.A. Baum, and C.C. Habeger, *Tappi J.*, **63**(2), 163-166 (1980).
- 7 G.A. Baum, D.C. Brennan, and C.C. Habeger, *Tappi J.* **64**(8), 97-101 (1981).
- 8 G. A. Baum, *Appita* **40**, 288-294 (1987).
- 9 Y. Pan, C. Habeger, and J. Biasca, *Tappi J.* **72**(11), 95-100 (1989).
- 10 C.C. Habeger and W.A. Wink, *Ultrasonics* **28**, 52-53 (1990).
- 11 C.C. Habeger, Private Communication.
- 12 M.S. Hall, *Sensors* **7**(7), 13-20 (1990).
- 13 P.H. Brodeur and M.S. Hall, *Ultrasonics Inter. 91 Conf. Proc.*, Butterworth-Heinemann, Oxford, 331-334 (1991).
- 14 W. A. Wink and G.A. Baum, *Tappi J.*, **66**(9), 131-133 (1983).
- 15 W. Sachse and Y.-H. Pao, *J. Appl. Phys.* **49**(8), 4320-4327 (1978).
- 16 C.C. Lee, M. Lahham, and B.G. Martin, *IEEE Trans. Ultra. Ferro. Freq. Contr.* **37**(4), 286-294 (1990).
- 17 M. O'Donnell, E.T. Jaynes, and J.G. Miller, *J. Acoust. Soc. Am.*, **69**(3), 696-701 (1981).
- 18 B. Castagnede, R.E. Mark, and Y.B. Seo, *J. Pulp Paper Sci.*, **15**(6), J201-J205 (1989).